Critical Behavior of O_2^- Ions in Ar Gas[1]

A.F.Borghesani[2,3], D.Neri[2], and A.Barbarotto[2]

---

[1] Paper presented at the Thirteenth Symposium on Thermophysical Properties, June 22-27, 1997, Boulder, Colorado, U.S.A.

[2] Istituto Nazionale per la Fisica della Materia, Dipartimento di Fisica "G. Galilei", University of Padua, Via F.Marzolo, 8, I-35131 Padua, Italy

[3] To whom correspondence should be addressed.

ABSTRACT

We measured the drift mobility of O_2^- impurity ions in Argon gas close to the critical point for $(151.5 < T < 157)\,K$ above $T_c = 150.86\,K$ and in the density range $(0.2 < N < 14.0) atoms\,nm^{-3}$ around $N_c = 8.08\,atoms\,nm^{-3}$. The density–normalized zero–field mobility $\mu_0 N$ of the ions shows a deep minimum as a function of N as $T \to T_c^+$. This anomalous reduction of $\mu_0 N$ occurs at a density $N_m \approx 0.8 N_c$. We believe that this behavior is due to the strong electrostriction exerted by the ion on the highly compressible gas. By introducing suitable contributions to the effective ion radius R due to large gas compressibility, the hydrodynamic Stokes formula $\mu_0 = e/6\pi\eta R$ is in good agreement with the experimental data.

KEY WORDS: electrostriction; hydrodynamic drag; ion drift mobility; kinetic theory.

1. INTRODUCTION

The motion of ions in fluids has been extensively studied to obtain information about the interaction between ions and atoms. In low density gases the ion–atom interaction potential can be determined from drift mobility data by using kinetic theory [1], while the mobility of ions in liquids is determined by the microscopic behavior and structure of the host fluid and can be described in terms of hydrodynamics [2].

The same attention has not been devoted to dense gases, where the density can be varied in a large interval so as to investigate the limits of applicability of either the kinetic or hydrodynamic description of the ionic motion. Moreover, there is a lack of investigations of the ion transport mechanisms near the liquid–vapor critical point [3,4] where the transport coefficients show an anomalous behavior due to critical fluctuations [5].

Positive ionic species (daughter ions in parent fluids) have been more carefully studied than negative ones because the former are easily produced by ionizing the medium. Their structure and transport properties are fairly well known. Electrostriction exerted by the ion strong electric field on the polarizable medium enhances the local density around the ion. The attraction strength increases with increasing the atomic polarizability, α, of the host atoms and with decreasing temperature T and can be so strong that the liquid may even locally solidify [6] or the ion can be surrounded by a solvation cluster. In this case, the ion transport is primarily determined by the hydrodynamic interaction of the large structure surrounding the ion with the fluid and is independent of the ionic species.

On the other hand, impurity negative ions are not equally well known. A very important species is O_2^- because O_2 is a very common impurity in gases and ions are produced by electron attachment [7]. The O_2^- mobility μ in dense gases has been studied as a function of N in ^{4}He at $T = 77\,K$ [8,15] but in

the neighborhood of the critical point only in Ne at $T = 45\,K \approx T_c + 0.6\,K$ in an extended density range $0.1 \leq N/N_c \leq 1.7$ [4], with N_c the critical density. In Ne $\mu_0 N$ shows a complicated behavior. At first, $\mu_0 N$ shows a broad maximum for $N \approx 6.0\,atoms\,nm^{-3}$. Then, it has a broad and shallow miminum for $N \approx (12-13)\,atoms\,nm^{-3} < N_c = 14.44\,atoms\,nm^{-3}$. Finally, it increases linearly for $N \geq N_c$ saturating for $N > 20.0\,atoms\,nm^{-3}$ to a constant value twice as large as the low density value.

In neither papers [4,8] the observed dependence of $\mu_0 N$ on N was satisfactorily explained. In the case of Ne [4] it was assumed that at high–N μ_0 might be described by the hydrodynamic Stokes's formula

$$\mu_0 = \frac{e}{6\pi\eta R} \tag{1}$$

where η is the gas viscosity and R is the radius of the ion. Electrostriction effects were taken into account by solving the Navier-Stokes equation in presence of the spatial nonuniformities surrounding the ion [9] yielding $\mu_0 = e/6\pi\eta FR$. The correction factor $F \approx 1$ depends on N and T as well as on the shape of the N and η profiles. FR can be considered as the effective ion radius. In any case, the agreement with the experimental data is quite poor.

One more unsolved question raised by the Ne–O_2^- experiment [4] is the absence of any anomalous behavior of $\mu_0 N$ for $N \approx N_c$ even though T_c was approached quite closely $\epsilon = (T - T_c)/T_c \approx 1.3 \times 10^{-2}$. A similar absence of anomalous behavior of μ_0 was observed for $^3He^+$ in ^3He close to T_c [10], where μ_0 shows a smooth reduction of less than 50 % for $\epsilon \geq 10^{-3}$ with the maximum mobility defect occuring for $N \approx 0.9\,N_c$.

On one hand, the Nernst–Einstein–Townsend relationship between μ_0 and the diffusion coefficient $D = (k_B T/e)\mu_0$ predicts an anomalous reduction of μ_0 at the critical point due to the anomalous behavior of the diffusion coefficient [5] but there is no experimental evidence [4,10]. On the other hand,

the experiments seem to confirm the theoretical prediction of Watanabe [11]. In this theory heavy ions, interacting with the atoms of the medium through a contact potential, should not be elastically scattered off long–wavelength fluctuations. Ions are not coupled to critical fluctuations because the relevant length scales (the correlation length ξ of fluctuations and the thermal wavelength of ions $\lambda_T \approx 0.02\,nm$) are too different. Moreover, the ionic thermal velocity is such that the time spent going through a fluctuation is much less than the fluctuation decay time so that the dissipative properties of the fluctuations do not influence μ_0.

It has been proposed recently [12] that the quantum nature of the interaction between the gas atoms and the additional electron in the O_2^- ion must be taken into account to describe structure and mobility of the ion. The electron is weakly bound in the ion and its orbit is extended in space. The competition between short–range repulsive exchange forces and the long–range polarization ion–atom interaction gives origin to a hollow cavity around the ion surrounded by a region of enhanced gas density. The strength of this enhancement is related to the polarizability of the gas atoms and to the gas compressibility χ_T and is very relevant close to the critical point.

This model [12] describes well μ_0 in the high–T, low–N case of He gas [8] where α is so low that only an empty void surrounds the ion. However, it fails in the case of the high–N, low–T Ne case [7] where the strong density enhancement around the ion cannot be neglected. The experimental data are reproduced almost quantitatively for high densities ($N > N_c$) by assuming the validity of the Stokes equation (1), by taking the position of the maximum of the density profile as the hydrodynamic ion radius R, and by using the viscosity η evaluated at the maximum density. However, the data for $N \leq N_c$ are not even qualitatively reproduced. We have therefore carried out measurements of the mobility of O_2^- ions in Ar to check some of

the issues raised in previous experiments and models. We have chosen Ar because polarization forces are very strong and no hollow cavity is expected to surround the ion. Moreover, the atomic polarizability of Argon is very large ($\alpha = 1.83 \times 10^{-40}\, Cm^2/V$) and the density enhancement around the ion should be very important. Therefore, Ar should represent a valid test of the predictions of Watanabe. We will show that $\mu_0 N$ of O_2^- ions in Ar gas is strongly affected by the critical point trough the formation of a thick layer of correlated fluid around the ion. Preliminary results have been recently published [13].

2. EXPERIMENTAL DETAILS

We used the same pulsed electron photoinjection technique [14] exploited for mobility measurements of O_2^- ions in Ne and He [4,15]. We refer to literature for details. The cell containing the gas (Ar "N60") is thermoregulated within $\pm 0.01\, K$. Thermal gradients are estimated to be $< 2\, K/m$. T is measured with a calibrated Pt resistor. The absolute value of T is known within $\pm 0.3\, K$. N is calculated from the pressure P and T by means of the equation of state of Gosman *et al.*[16].

Two parallel–plate, gold–plated brass electrodes in the cell are separated by a distance $d = 10\, mm$. A short U.V. light pulse impinging on the photocathode extracts electrons that are captured by O_2 impurities to form O_2^- ions. The current induced by the ion motion towards the anode is integrated by a RC network, amplified, and recorded by a digital scope. The signal waveform is processed by a P.C. to obtain the ionic drift time τ_i. μ is calculated from the relationship $\mu = d^2/\tau_i V$, where V is the applied voltage. The relative accuracy of μ is estimated to be $\approx 5\%$.

3. EXPERIMENTAL RESULTS AND DISCUSSION

For electric fields up to $0.3 MV/m$, and for every T and N, μ is practically field independent, equal to its zero–field value μ_0, as shown in Fig. 1, because

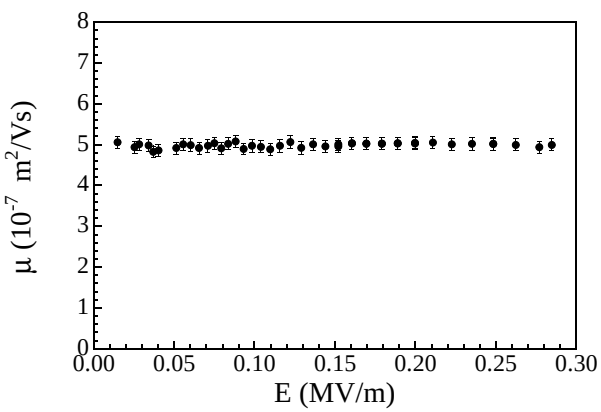

Figure 1: Electric field dependence of the O_2^- ion mobility μ for $N = 5.83\, atoms\, nm^{-3}$ at $T = 154\, K$.

the ions are near thermal equilibrium with the gas atoms. In Figs. 2 and

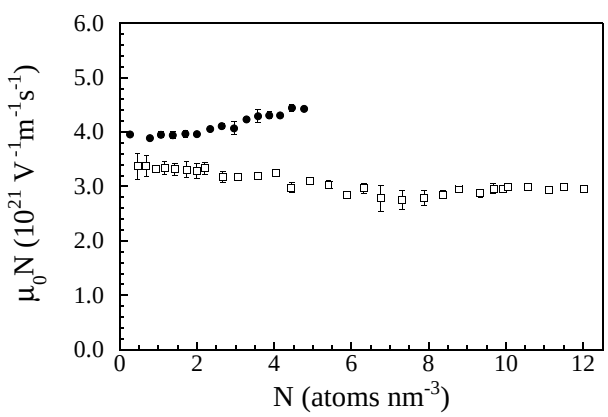

Figure 2: Density–normalized zero–field mobility $\mu_0 N$ as a function of N for $T = 180\, K$ (closed dots) and for $T = 157\, K$ (open squares).

3 $\mu_0 N$ is shown as a function of N for several values of T. As $T \to T_c$ the behavior of $\mu_0 N$ changes greatly. For $T \approx 180\, K \gg T_c$, $\mu_0 N$ increases linearly with N. This behavior is very similar to that shown in He [8,15] and in Ne [4,15]. For $T = 157\, K \approx T_c + 6\, K$ ($\epsilon \approx 4 \times 10^{-2}$) the slope changes sign and $\mu_0 N$ decrases linearly with N. For $T = 154\, K$ ($\epsilon \approx 2 \times 10^{-2}$) $\mu_0 N$ has a broad minimum in the density range $(5.5 < N < 8) \times\, atoms\, nm^{-3}$. Finally,

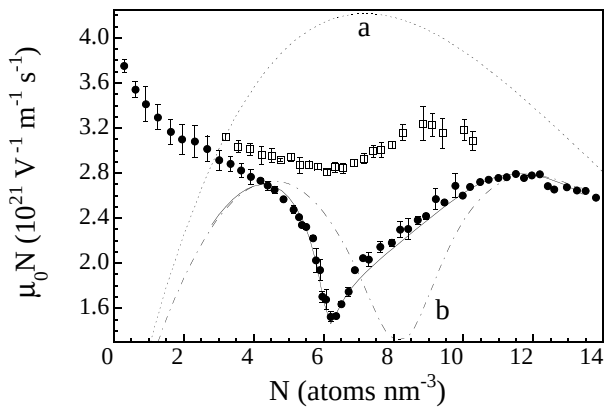

Figure 3: $\mu_0 N$ as a function of N for $T = 154\,K$ (open squares) and for $T = 151.5\,K$ (closed dots). Curve a is the prediction of Eq.(1). Curve b is the prediction of Eq.(1) with R given by Eq.(2). The solid curve is the prediction of Eq.(1) with R given by Eq. (4).

for $T = 151.5 \approx T_c + 0.6\,K$ ($\epsilon \approx 4 \times 10^{-3}$) $\mu_0 N$ has a very deep minimum located at $N = N_m \approx 6.5\,atoms\,nm^{-3}$. It is evident that the mobility drop for $T \to T_c$ has to be connected with the approach to the critical point where both χ_T and η diverge, but it is surprising that the strongest effect appears for $N < N_c$.

Owing to the relationship among μ_0, diffusion coefficient D, and drag coefficient of a sphere of radius R and charge e, $D = k_{\rm B}T/6\pi\eta R = (k_{\rm B}T/e)\mu_0$, known to be valid even for microscopic particles [17], μ_0 data could be used to determine η. However, the determination of the anomaly of η in binary mixtures at the critical point from measurements of the diffusion coefficient of Brownian particles yields controversial results according to the degree of interaction of the particles with the liquid [18]. To obtain agreement with standard viscometric measurements it has to be assumed that the particles are surrounded by a layer of correlated fluid enhancing their radius. The layer thickness is $\delta \propto \xi$ and depends on the interaction of the particles with the fluid.

In the present case there is a strong interaction between the ion and the highly polarizable medium and electrostriction plays an important role. We

believe that μ_0 is more sensitive to the divergence of χ_T that determines the electrostriction strength rather than to the weak divergence of η [19]. Thus,

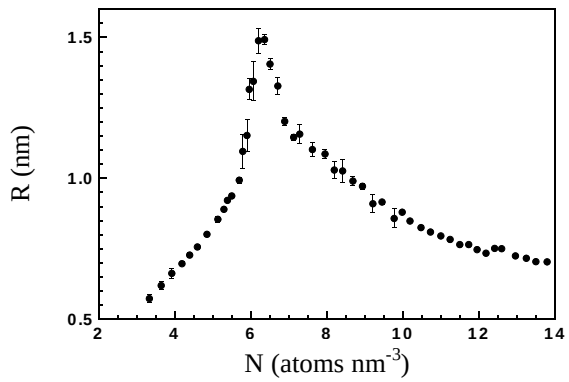

Figure 4: Hydrodynamic ion radius R calculated from from $\mu_0 N$ by means of Eq. (1) for $T = 151.5\,K$.

by assuming the validity of Eq. (1), the hydrodynamic ion radius R is obtained by inverting the $\mu_0 N$ data. We used η values as function of N found in literature [20]. In Fig. 4 we show R as a function of N for $T = 151.5\,K$. It has a sharp maximum for N_m where $\mu_0 N$ is minimum. For $N \approx 3.0\,atoms\,nm^{-3}$, $R \approx 0.5\,nm$ close to the value $R_1 \approx 0.46\,nm$ of a complete solvation shell of Ar atoms surrounding the ion (the Ar–Ar interaction hard–core radius is $\sigma_A = 0.34\,nm$ and that of the O_2^-–Ar interaction can be estimated to be $\sigma_O \approx 0.29\,nm$ [21]). For $N \approx 14.0\,atoms\,nm^{-3}$ $R \approx 0.76\,nm$ close to the value $R_2 \approx 0.82\,nm$ corresponding to two completely developed solvation

shells.

In order to explain the sharp maximum of R for $N = N_m$ we assume that a correlated fluid layer is dragged along by the ion thus increasing its effective radius. In the critical region of Ar the correlation length can be cast in the form $\xi = L\left[S\left(0\right)\right]^{1/2}$ where $L \approx 0.316\,nm$ is the short–range correlation length and $S(0) = Nk_{\mathrm{B}}T\chi_T$ is the long–wavelength limit of the static structure factor. We therefore put

$$R = (a_0 + a_1 N) + a_2\sqrt{S\left(0\right)} \tag{2}$$

where a_0, a_1, and a_2 are fitting parameters. The linear part $(a_0 + a_1 N)$ interpolates between the radii of one and two solvation shells, while the term $\propto \sqrt{S(0)}$ is relevant close to the critical point and takes into account the thickness of the correlated fluid layer. By using Eq.(2) we obtain curve b in Fig. 2. The $\mu_0 N$ minimum occurs for $N = N_c$, where $S(0)$ is maximum, and not for $N = N_m$. The reason of the discrepancy is due to the fact that $S(0)$ is a thermodynamic property of the unperturbed gas and we have not yet considered the perturbation induced by electrostriction.

This enhances the local density N_r around the ion (and, hence, also the local viscosity $\eta_r \equiv \eta(N_r)$) so that N_r takes on the value N_c at a given distance r from the ion only if $N < N_c$, where N is the unperturbed gas density. At the same distance the local value of the static structure factor $S_r \equiv S(0, N = N_r)$ is obviously maximum. This fact suggests that the fluid properties determining the ion transport are not those of the unperturbed fluid. The density profile is calculated according to the electrostriction model [6] by numerically inverting the following equation

$$-V\left(r\right) = K^2\left(N_r\right)\int_N^{N_r}\left(\frac{\partial P}{\partial N}\right)_T \mathrm{d}\ln N \tag{3}$$

where $V(r)$ is the ion–atom interaction potential, and K is the dielectric constant of the gas. A typical density profile is shown in Fig. 5 [13]. For

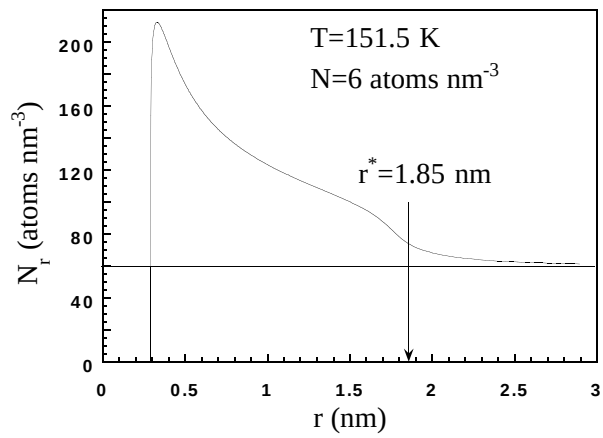

Figure 5: Electrostriction induced density profile for $N = 6\,atoms\,nm^{-3}$ and $T = 151.5\,K$. A 12–6–4 potential with a hard–core radius $\sigma = 0.29\,nm$ and a well depth of $1.57 \times 10^{-20}\,J$ has been used.

a given N, S_r differs from $S(0)$ and is maximum at the distance r where $N_r = N_c$. The optimum value $r^\star$ of r has been determined by imposing that S_r is maximum for $N = N_m$, yielding $r^\star = 1.85\,nm$. Accordingly, in Eq. (1) we used the local value of η, evaluated at the same distance from the ion $r^\star = 1.85\,nm$ for every N and adjusted the parameters in Eq. (2) so as to fit the data, yielding

$$R = 0.475 + 1.143 \times 10^{-3} N + 0.066\sqrt{S_r} \tag{4}$$

with R in nm and N in units of $atoms\,nm^{-3}$. The results of this model are shown as the solid line in Fig. 2. The agreement of this modified Stokes formula with the data is very good, even for quite low N ($N \approx 4.0\,atoms\,nm^{-3}$).

In the same Fig. 2 we also show the results of Eq. (1) (curve a) obtained by using the unperturbed gas viscosity and an effective radius including only the linear contribution $R = 0.475 + 1.143 \times 10^{-3} N$. The striking disagremeent with the data puts into clear evidence the relevance of the contribution of the layer of correlated fluid to the effective ionic radius and the importance of using local values for the fluid properties. As seen in Fig. 4, it is always $R < r^\star$ the distance where the fluid properties must be evaluated. This casts some doubts on the simple picture of a solid–like sphere of radius R,

where no–slip boundary conditions apply, since R and η in Eq. (1) are determined by the properties of the unperturbed fluid at distances $r^\star > R$. In any case, the agreement of the electrostricton model with the data supports the conclusion that μ_0 is more sensitive to χ_T than to η, because of the strong ion–atom polarization interaction and of the critical divergence of χ_T, much stronger than that of η. These results, moreover, indicate that the use of a contact potential in the theory of Watanabe is a very bad approximation.

Finally, we point out that the hydrodynamic description of the ionic mobility fails for $N \leq 4.0\, atoms\, nm^{-3}$, where it is evident that a different transport mechanism is active. A more detailed theoretical analysis of the momentum transfer mechanisms in the transition regime from kinetics–to hydrodynamics is still needed to fully describe the density dependence of the ion mobility.

REFERENCES

1. E. A. Mason and E. W McDaniel,*Transport Properties of Ions in Gases*, (Wiley, New York, 1988).

2. H. T. Davis, S. A. Rice, and L. Meyer, J. Chem. Phys. **37**: 947 (1962).

3. N. Gee, S.S.–S. Huang, T. Wada, and G. R. Freeman, J. Chem. Phys. **77**: 1411 (1982).

4. A. F. Borghesani, D. Neri, and M. Santini, Phys. Rev. **E 48**: 1379 (1993).

5. K. Kawasaki and J. D. Gunton, *Critical Dynamics* in *Progress in Liquid Physics*, C. A. Croxton ed., (Wiley, New York, 1978), p. 175

6. K. R. Atkins, Phys. Rev. **116**: 1339 (1959).

7. A. K. Bartels, Phys. Lett. **45 A**: 491 (1973).

8. A. K. Bartels, Appl. Phys., **8**: 59 (1975).

9. R. M. Ostermeier and K. W. Schwarz, Phys. Rev. **A 5**: 2510 (1972).

10. R. Cantelli, I. Modena, and F. P. Ricci, Phys. Rev. **171**: 236 (1968).

11. S. Watanabe, J. Phys. Soc. (Japan) **46**: 1819 (1979).

12. K. F. Volykhin, A. G. Khrapak, and W. F. Schmidt, J.E.T.P. **81**: 901 (1995).

13. A. F. Borghesani, D. Neri, and A. Barbarotto, Chem. Phys. Lett. **267**: 116 (1997).

14. A. F. Borghesani, L. Bruschi, G. Torzo, and M. Santini, Rev. Sci. Instrum. **57**: 2234 (1986).

15. A. F. Borghesani, F. Chiminello, D. Neri, and M. Santini, Int. J. Thermophys. **16**: 1235 (1995).

16. A. L. Gosman, R. D. McCarty, and J. G. Hust, Natl. Bur. Stand. Rep. No. 27 (U.S.G.P.O., Washington, D.C., 1969).

17. G. L. Pollack, Phys. Rev. **A 23**: 2660 (1981).

18. K. B. Lyons, R. C. Mockler, and W. J. O'Sullivan, Phys. Rev. Lett. **30**: 42 (1973).

19. R. F. Berg and M. R. Moldover, J. Chem. Phys. **93**: 1926 (1990).

20. N. J. Trappeniers, P. S. van der Gulik, and H. van den Hooff, Chem. Phys. Lett. **70**: 438 (1980).

21. G. C. Maitland, M. Rigby, E. B. Smith, and W. A. Wakeham, *Intermolecular Forces. Their Origin and Determination* (Clarendon Press, Oxford, 1981).